Journal of Magnetic Resonance **151,** 129–135 (2001)
doi:10.1006/jmre.2001.2337, available online at http://www.idealibrary.com on IDEAL®

COMMUNICATIONS

Slow-Down of ^{13}C Spin Diffusion in Organic Solids by Fast MAS: A CODEX NMR Study

D. Reichert,* T. J. Bonagamba,†,‡ and K. Schmidt-Rohr‡,[1]

*FB Physik, Martin-Luther Universität Halle-Wittenberg, 06108 Halle, Germany; †Instituto de Física de São Carlos, Universidade de São Paulo, Caixa Postal 369, CEP 13560-970 São Carlos, SP, Brazil; and ‡Department of Chemistry and Ames Laboratory, Iowa State University, Ames, Iowa 50011

Received August 29, 2000; revised March 30, 2001; published online May 18, 2001

One- and two-dimensional ^{13}C exchange nuclear magnetic resonance experiments under magic-angle spinning (MAS) can provide detailed information on slow segmental reorientations and chemical exchange in organic solids, including polymers and proteins. However, observations of dynamics on the time scale of seconds or longer are hampered by the competing process of dipolar ^{13}C spin exchange (spin diffusion). In this Communication, we show that fast MAS can significantly slow down the dipolar spin exchange effect for unprotonated carbon sites. The exchange is measured quantitatively using the centerband-only detection of exchange technique, which enables the detection of exchange at any spinning speed, even in the absence of changes of isotropic chemical shifts. For chemically equivalent unprotonated ^{13}C sites, the dipolar spin exchange rate is found to decrease slightly less than proportionally with the sample-rotation frequency, between 8 and 28 kHz. In the same range, the dipolar spin exchange rate for a glassy polymer with an inhomogeneously broadened MAS line decreases by a factor of 10. For methylene groups, no or only a minor slow-down of the exchange rate is found.

INTRODUCTION

Slow molecular processes with rates $k = 1/(2\tau_c)$ on the order of 10^3/s down to less than 0.1/s play an important role in the materials properties of synthetic polymers (*1, 2*), the function of biopolymers (*3*), transport of small molecules in zeolites (*4, 5*), or structure–property relationships in food-related materials (*6*). Solid-state exchange nuclear magnetic resonance (NMR) measuring segmental reorientations (*2, 7–11*) is a powerful tool for studying such processes since it provides information about the time constants as well as the geometry of the segmental motions with high selectivity. In particular, 1D magic-angle spinning (MAS) exchange NMR methods (*12–17*) provide good signal intensity and site resolution.

A shortcoming common to all solid-state exchange experiments is that they cannot directly distinguish the effects of molecular dynamics and dipolar-coupling-induced spin exchange (also referred to as ^{13}C spin diffusion) (*18–23*). The only known way to achieve this is to vary the parameters that control the rates of the exchange processes. For example, in experiments at different temperatures one expects the rate of the motional process to change while the dipolar spin exchange processes remain nearly unaffected (*24*). However, even if one can tell the processes apart (*24–26*), spin diffusion prevents the detection of molecular motions with time constants close to or slower than those of the spin exchange. Dipolar ^{13}C spin exchange in organic solids at natural isotopic abundance becomes significant on a time scale of 0.5 to 5 s (*25–27*), with a strongly nonexponential profile (*28, 29*).

To extend the dynamic range of the experiments toward longer mixing times, one must decrease the rate of dipolar spin exchange. Methods for controlling the rate of ^{13}C spin diffusion have been the subject of many papers (for a review, see (*22*)). However, the main intention in most cases has been to speed up the spin exchange process, in order to use it in correlation experiments for structural studies. So far, no exchange experiment with reduced dipolar ^{13}C spin diffusion on the time scale of seconds has been successfully demonstrated.

Fast MAS suppresses the ^{13}C–^{13}C and ^{13}C–^{1}H dipolar couplings as well as instantaneous isotropic and anisotropic chemical shift differences that form the homogeneous Hamiltonian (*30*) responsible for ^{13}C spin diffusion. While more traditional MAS exchange NMR methods such as EIS (*12*), ODESSA (*13, 14*), and time-reversed ODESSA (*13, 14*) utilize the alteration of relative spinning sideband intensities due to the exchange processes and thus work well only for moderate MAS rotation speeds, the centerband-only detection of exchange (CODEX) technique can be performed at any MAS frequency (*15, 16*).

In this Communication, we show that CODEX NMR under fast MAS is a successful approach for performing exchange NMR that can characterize segmental reorientations, while reducing the efficiency of undesirable dipolar spin exchange between unprotonated carbons by means of the high spinning

[1] To whom correspondence should be addressed. E-mail: srohr@iastate.edu.

1090-7807/01 $35.00

speed. We have studied various ^{13}C-labeled model compounds to quantify the spinning-speed dependence of the spin exchange between chemically equivalent sites. This case is most relevant for dynamics studies using singly ^{13}C-labeled molecules or segments, where spin diffusion between the chemically equivalent labeled sites limits the detection of motions on the time scale of seconds (*24–26*).

THEORETICAL BACKGROUND

CODEX and fits of the mixing-time dependence. In a CODEX experiment, both exchange and reference data are acquired and compared for each mixing time. In this way, the influence of T_1 relaxation drops out and the resulting exchange intensity is normalized to values ranging from unity for $t_m \ll \tau_c$ down to $1/M$ for $t_m \gg \tau_c$. M is the number of sites accessible to the exchange process. For spin exchange, the distribution of exchange rates can be taken into account by replacing the exponential decay by a stretched exponential function (*29, 31*). The CODEX decay in the case of sufficiently long CODEX recoupling cycles ($\delta N t_R \gg 2\pi$, δ being the chemical shift anisotropy parameter and $t_R = 1/\nu_R$ the MAS rotation period) can thus be expressed as (*16*)

$$I(t_m) = \frac{1}{M} + \left(1 - \frac{1}{M}\right) \cdot e^{-(t_m/\tau^{SD})^{\beta}}, \qquad [1]$$

with the spin diffusion time constant τ^{SD} and the nonexponentiality parameter β. In a crystalline material, M is identical to the number of magnetically inequivalent sites per unit cell. For the amorphous polycarbonate, M approaches infinity because of the extremely large number of different relative orientations of two neighboring carbonate groups. In the fitting of the experimental decays, $1/M$ was kept fixed at its theoretical value, which provides a more reliable fit.

RESULTS AND DISCUSSION

Figure 1 shows cross-polarization/magic-angle spinning (CP/MAS) spectra for both the alanine–glycine mixture (a) and the polycarbonate–glycine mixture (b) (see Experimental for a description of the sample compositions; the powder mixtures of these ^{13}C-labeled compounds were prepared simply to measure several compounds simultaneously and thus reduce the experiment time; this also ensures identical experimental conditions for the components of a given mixture). In (a), the peaks (from low field) are due to ^{13}COO alanine, $^{13}CH_2$ glycine, and $^{13}CH_3$ alanine. The splitting of the glycine methylene signal into two peaks is due to two different crystal modifications (*32*): the line at ~43 ppm corresponds to the γ-form, while that at about 44 ppm is the signal of the α-modification. The different forms differ in the number of magnetically inequivalent molecules per unit cell, determined by crystallography, and thus in the number M in Eq. [1]: $M = 3$ for the γ- (*33, 34*), and $M = 2$ for the α-

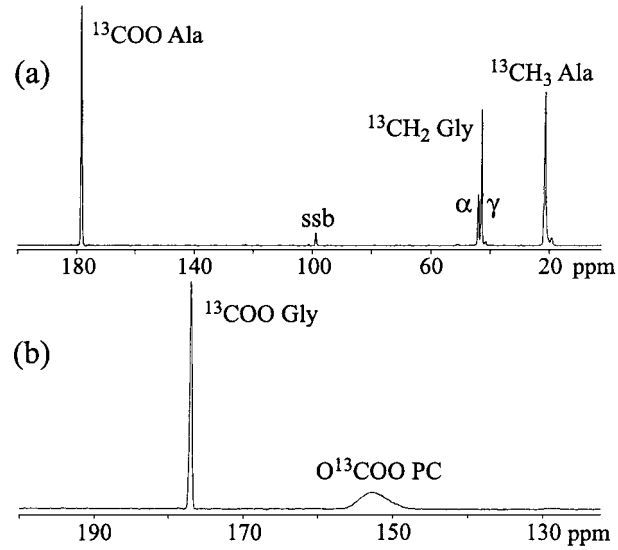

FIG. 1. CP-MAS spectra of the mixtures of (a) ^{13}COO alanine (Ala), $^{13}CH_2$–^{15}N glycine (Gly), and $^{13}CH_3$ alanine at a rotation speed of ν_R = 8 kHz; (b) 100% O^{13}COO-labeled polycarbonate (PC) and ^{13}COO glycine at $\nu_R = 28$ kHz. TPPM decoupling at $\gamma B_1/2\pi = 130$ kHz was applied. A total of 32 accumulations were added for each spectrum.

form (*35*). Since the T_1 of $^{13}CH_3$ alanine is only ~70 ms, reliable exchange decays could not be obtained for this methyl group and will not be discussed. The resonances in Fig. 1b are due to (from low field) ^{13}COO glycine and O^{13}COO polycarbonate (PC). Figure 2 shows CODEX decays for $^{13}CH_2$ glycine as well as the carboxyl carbons in unlabeled methylmalonic acid (upper right corner) in (a), O^{13}COO PC in (b), and ^{13}COO glycine in (c). To cover several orders of magnitude of the mixing time,

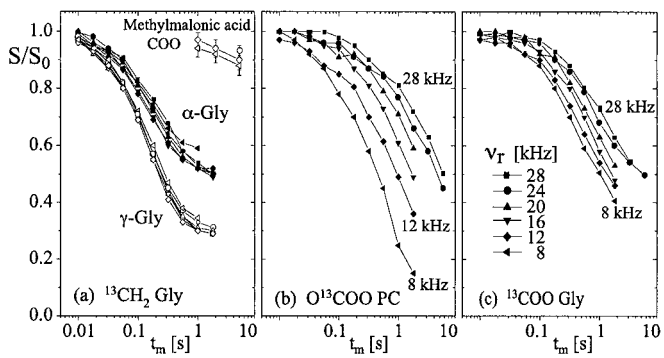

FIG. 2. CODEX decays S/S_0 (t_m) for (a) $^{13}CH_2$ glycine: α-(filled symbols) and γ-form (open symbols). Data for the COO site in unenriched methylmalonic acid are shown in the upper right corner, with rotation frequencies of 5 (◁), 10 (◇), and 25 kHz (○) at $Nt_R = 0.8$ ms. (b) O^{13}COO-Enriched polycarbonate. (c) ^{13}COO-Labeled γ-glycine. For the ^{13}C-enriched samples, Nt_R was set to 1 ms for (a) and to 0.5 ms for (b) and (c). Sample rotation frequencies for the ^{13}C-enriched samples of 8, 12, 16, 20, 24, and 28 kHz were used, with corresponding symbols indicated in (c). A total of 128 accumulations were added at each mixing time for both the exchange (S) and the reference (S_0) experiment, except for unenriched methylmalonic acid, which was measured with 576 and 5760 scans at 10 and 25 kHz, respectively.

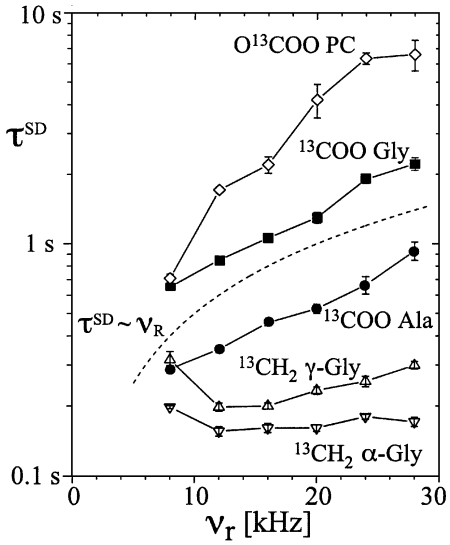

FIG. 3. Spin exchange times $\tau_{SD} = (k_{SD})^{-1}$ vs MAS rotation frequency ν_R for the five ^{13}C-enriched substances (four amino acids and polycarbonate) as indicated in the plot. The time constants τ_{SD} were extracted by fitting the CODEX decays of Fig. 2 with Eq. [1]. The dashed line is the function $\tau_{SD} = 5 \times 10^{-5} S^2 \nu_R$.

we have chosen a plot of intensity vs $\log(t_m)$. The time constant τ^{SD} of the spin diffusion process is close to the mixing time value at which the intensity drops down to $1/e$. It is obvious from Fig. 2 that the effect of the sample rotation rate is quite different for different types of carbons: it ranges from almost no effect (^{13}CH$_2$ glycine) to a slow-down of the spin diffusion by almost one order of magnitude (PC). In order to enable a more detailed discussion, we fitted all decays with Eq. [1] and plotted the extracted ^{13}C spin diffusion time constants τ^{SD} as a function of the MAS rotation frequency in Fig. 3. The non-exponentiality parameter β ranges between 0.7 and 0.8, except for the α-carbons in glycine, where it is around 0.9 for ^{13}CH$_2$ in γ-glycine and close to 1.0 for ^{13}CH$_2$ in α-glycine.

For the unenriched methylmalonic acid, the data shown in the upper right corner of Fig. 2a exhibit a significant shift to the right, which shows a marked slow-down of spin exchange with increasing rotation speed. However, sensitivity and experimental time did not permit the measurement of more complete spin diffusion curves; therefore, we will discuss only the data from the ^{13}C-enriched substances in more detail.

Discussion of ^{13}C spin diffusion. To discuss the different behavior of the spin diffusion time constant τ^{SD}, we divide the five different types of carbons into three groups. The carboxyl carbons in ^{13}COO alanine and ^{13}COO glycine are typical examples of unprotonated chemically equivalent carbons, while the α-carbons in the two ^{13}CH$_2$ glycines are examples for strongly ^{1}H-coupled carbons. Last, the 500-Hz inhomogeneously broadened resonance of PC represents a distribution of isotropic chemical shifts due to conformational effects in the amorphous polymer. Thus, this substance is an example for spin exchange between slightly chemically nonequivalent carbons.

Since the spin exchange under the present conditions involves the direct ^{13}C–^{13}C coupling as well as the ^{1}H–^{13}C and ^{1}H–^{1}H couplings, a quantitative description is complicated and beyond the scope of this Communication. Spin dynamics simulations might provide deeper insight. However, it is expected that at least for the strongly coupled α-carbons, the ^{1}H–^{1}H couplings play a major role; thus, more spins may have to be considered than can currently be handled in rigorous calculations. Therefore, we will restrict ourselves to a qualitative discussion.

Several cases of spin exchange have been treated in the literature. A common one is proton-driven spin diffusion (*18, 22, 36*). In this case, the coupling of the ^{13}C's to protons, as indicated by the undecoupled homogeneous ^{13}C linewidth, is much larger than the ^{13}C–^{13}C dipolar coupling. The spin diffusion rate is then proportional to the overlap integral of the lines of the exchanging ^{13}Cs, which increases with decreasing linewidth (*18, 22, 23, 36*).

Spin exchange between chemically equivalent spins. A more tractable case is exchange between chemically equivalent proton-decoupled ^{13}C sites, first treated by Maricq and Waugh (*30*) and sometimes considered "$n = 0$ rotational resonance" (*37*). Chemically equivalent spins (more generally, spins in the strong coupling limit of $|\omega_{iso}^A - \omega_{iso}^B| < \omega_{dipol}^{AB}$) with different chemical shift tensor orientations, i.e., magnetic inequivalence, exchange magnetization with a rate that is proportional to $D \cdot \Delta\sigma/\nu_R$, D being the dipolar coupling and $\Delta\sigma$ the instantaneous isotropic and anisotropic chemical shift difference (*30*), which reflects the difference in orientation of the interaction chemical shift tensors (*30*). Even though the dipolar coupling is much smaller than the rotation speed and the isotropic chemical shift difference is zero, MAS does not "spin out" the dipolar coupling up to very high rotation frequencies. The sum of the instantaneous anisotropic chemical shift difference and the dipolar coupling does not commute with itself at different rotor orientations, i.e., they form a homogeneous Hamiltonian in the sense of Maricq and Waugh (*30*). Thus, the anisotropy effect after a full rotation period does not vanish. It increases proportional to the dipolar coupling D and the instantaneous chemical shift difference $\Delta\sigma$.

For this description to be applicable, the ^{1}H–^{13}C coupling must be negligible. This is the case when sufficiently strong proton decoupling is applied during the mixing time. It also holds if the effective C–H coupling under MAS is smaller than the ^{13}C–^{13}C dipolar coupling responsible for the spin exchange; this can be achieved for unprotonated carbons by fast sample rotation. The linewidths plotted in Fig. 4 show that this is indeed the case for the COO carbons at rotation speeds above $\sim$15 kHz.

The essential dependence for our consideration is the dependence of the spin exchange rate $1/\tau_{SD}$ on $1/\nu_R$, the inverse of the rotation frequency. It can be seen from Fig. 3 that the carboxylic carbons in ^{13}COO alanine and ^{13}COO glycine fit the expected dependence $\tau^{SD} \sim \nu_R$ relatively well for high rotation

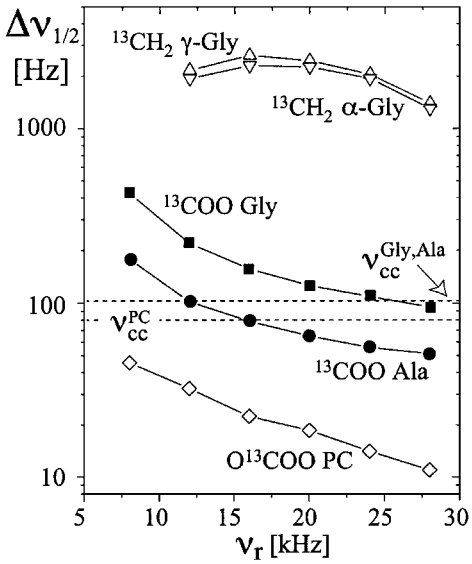

FIG. 4. Linewidths of ^{13}C resonances without ^{1}H decoupling. The symbols match those in Fig. 3. For ^{13}COO–alanine and ^{13}COO–glycine, it was determined by measuring the linewidth in undecoupled CP/MAS spectra; otherwise, it was determined by rotor-synchronized Hahn-echo experiments without ^{1}H decoupling during the echo delays. Due to longer Hahn-echo delays for slower rotation frequencies, the first CH_2 data points of Δ and ∇ were obtained from two delays only; thus, they have a larger uncertainty, which might explain the unexpected drop for the lowest rotation speed. Dashed lines indicate the strongest relevant ^{13}COO–^{13}COO dipolar coupling in alanine, glycine, and polycarbonate, as determined from the crystal structures and from NMR data.

speeds. To show the shape of this dependence, we have plotted the dashed line $\tau^{SD} = 10^{-5} S^2 \nu_R$ for comparison. The difference in the absolute values for τ^{SD} for alanine and glycine is probably due to the different distances and relative ^{13}COO-group orientations in their crystal structures, i.e., due to differences in D and $\Delta\sigma$.

Effects of homogeneous C–H linewidth. At smaller speeds, the change in the spin exchange time constant with ν_r is slowed down by a counteracting effect: The line narrowing with increasing rotation speed observed in Fig. 4 leads to a more efficient resonance overlap with increasing ν_R, which according to the theory of proton-driven spin diffusion increases the spin diffusion rate (*18, 22, 27*). As a result, the increase of τ^{SD} with ν_R at slower rotation speeds is less steep than the ν_R-proportional curve.

For the strongly ^{1}H-bonded CH_2 carbons in glycine, proton-driven spin diffusion will lead to efficient spin exchange (shorter τ^{SD}), as we indeed observed experimentally. The dependence of the spin-diffusion rate on the rotation frequency is only weak. This can be understood from the presence of strong ^{13}C–^{1}H and ^{1}H–^{1}H couplings that are not considered in the theory of Maricq and Waugh (*30*). These couplings are reflected in the widths of the undecoupled ^{13}C resonances. For ^{13}COO glycine and ^{13}COO alanine, we measured the linewidth from CP-MAS spectra that were acquired without ^{1}H decoupling. Since this is not possible for the α-carbons and the carboxyl carbon in PC due to spectral overlap and distribution of isotropic chemical shifts, respectively, we performed rotor-synchronized Hahn-echo experiments for these compounds (without ^{1}H decoupling during the echo delays). The results are plotted in Fig. 4. The much larger linewidths of the CH_2 carbons, compared to those of the carboxylic carbons, confirm the presence of stronger ^{1}H–^{13}C and ^{1}H–^{1}H couplings. A more detailed discussion would require an extensive theoretical treatment and/or extensive spin dynamics simulation and is beyond the scope of this Communication.

Spin exchange between chemically inequivalent sites. The strongest effect of the rotation speed on the spin exchange time constant is seen for the O^{13}COO-labeled PC. It again represents weakly ^{1}H-coupled ^{13}C spins but in contrast to the case of ^{13}COO alanine and ^{13}COO glycine, the exchange now happens between slightly chemically inequivalent spins. Since the maximum isotropic chemical shift difference is comparable to, and the ^{13}C–^{1}H dipolar coupling is always smaller than, the ^{13}C–^{13}C dipolar coupling, this case represents a good example for the theory of Maricq and Waugh (*30*). Indeed, the dependence of the spin exchange time constant qualitatively fits the expected dependence on the rotation frequency $\tau_D \sim \nu_R$. This result obtained for PC is expected to be generally relevant for exchange NMR investigations of unprotonated sites in amorphous polymers. The results shown here indicate that the application of fast MAS in exchange experiments will extend the applicability of such experiments considerably. Given that the overall dynamic range of MAS exchange studies of molecular dynamics covers about three frequency decades so far, gaining one additional frequency decade by efficiently suppressing spin diffusion provides an extension of the dynamic range for the observation of molecular motions by about one-third.

SUMMARY AND OUTLOOK

Combining fast MAS and the recently introduced CODEX technique, we have studied the spinning-speed dependence of the rate of ^{13}C spin exchange. Quantitative experiments were performed using singly ^{13}C-labeled compounds. The data show that it is possible to reduce the rate of dipolar ^{13}C spin exchange between chemically equivalent unprotonated nuclei approximately inversely proportional to the rotation speed. For unprotonated chemically inequivalent sites, the reduction may be even stronger. A fourfold increase in rotation frequency, to 28 kHz, reduced the spin diffusion rate in O^{13}COO-labeled polycarbonate, where the ^{13}C-labeled sites are slightly chemically inequivalent, by a factor of 10. Limited data of COO groups in unlabeled methylmalonic acid also showed a measurable slowdown of spin exchange. On the other hand, the proton-driven spin diffusion between CH_2 groups was not strongly dependent on the rotation speed, up to the maximum of 28 kHz used here. These results are expected to also apply for studies of slow dynamics using other important nuclei like ^{15}N (*17*). Although the use of fast MAS requires small MAS rotors with limited sample

volume, this is in part compensated by the better radiofrequency performance of such probes. Also, for partially enriched substances the necessary minimum number of 128 accumulations, as required for complete phase cycling, may be already sufficient for a reasonable signal-to-noise ratio, as we have shown for the singly labeled amino acids. We anticipate that further developments in probe technology will enable even higher rotation speeds (*38*) so that the disturbing effect of dipolar ^{13}C spin exchange in MAS studies of slow dynamics can be further reduced.

EXPERIMENTAL

NMR parameters. Experiments were performed on a DSX400 spectrometer using a Bruker 2.5-mm MAS probe. Typical ^{13}C 90° pulses were 2.5 μs, and ^{1}H-TPPM (two-pulse phase modulation) decoupling fields of 130 kHz were applied. Constant amplitude cross polarization at the (−1) spinning sideband of the matching condition was used, with a Hartmann–Hahn match carefully adjusted for each MAS spinning frequency.

The CODEX technique is a 1D MAS exchange method that works well under the conditions of fast MAS (*15, 16*). It is based on a stimulated echo generated by the anisotropic chemical shift which is recoupled before and after the mixing time by trains of two 180° pulses per rotation period. The recoupling efficiency depends only on the total time of recoupling (*16*) and can be matched easily for different rotation frequencies. Under conditions of fast spinning, transverse relaxation is very slow; therefore, it is necessary to extend the original phase cycle for proper cancellation of transverse magnetization that has survived the z-periods, not only the mixing time t_m but also the second z-period t_z. For the convenience of the reader, we provide this phase cycle in the Appendix.

It must be noted that recoupling of dipolar interactions to fast-relaxing heteronuclei (for example, ^{14}N) will result in additional exchange (*39, 40*). In amino acids, this relaxation-induced dipolar exchange with recoupling (RIDER) effect (*39*) is largest for α-carbons since they are directly bonded to nitrogen. For that reason, the model substance for α-carbons, $^{13}CH_2$-labeled glycine, was also ^{15}N enriched. Since the T_1 of ^{15}N is longer than that of ^{14}N, the RIDER effect, which becomes effective only at long recoupling times Nt_r anyway (*39*), will be small, and we have neglected it in this work.

Samples. In compounds at natural ^{13}C abundance, the ratio of spin exchange rate and the relaxation time T_1 is often close to 1. Spin exchange is so slow that the duration of the mixing time, and thus the whole experiment, becomes very long, and the sensitivity is low. Therefore, precise data are difficult to obtain with such compounds. For this reason, we used mostly ^{13}C-labeled amino acids and a polymer in which the spin exchange rate is about one order of magnitude faster than in natural abundance, so that exchange decays can be acquired in reasonable experimental times. At ambient temperature and on the time scale of interest, these molecules or their building blocks containing the ^{13}C nuclei under investigation do not perform significant molecular motions.

We used two ^{13}C-labeled samples containing powder mixtures of five polycrystalline amino acids and one glassy polymer. The mixtures are not special in any way; they simply permitted us to reduce the experiment time, since the components in a given mixed powder are measured simultaneously. Each component can be clearly identified, based on its characteristic isotropic chemical shifts. Due to the large grain sizes in the powder mixtures, undesired spin exchange between the molecules of the different materials is completely insignificant. This approach also ensures identical measurement conditions for all components in the mixture. The first sample (alanine–glycine mixture) contains ^{13}COO alanine (1-^{13}C alanine), $^{13}CH_2$–^{15}N glycine (2-^{13}C, ^{15}N glycine), and $^{13}CH_3$ alanine (3-^{13}C alanine) (99% labeled, 4 mg of each); the other (polycarbonate–glycine mixture) consists of 9 mg of 100% O^{13}COO bisphenol-A polycarbonate and 1.3 mg ^{13}COO glycine (1-^{13}C glycine). Running through the minimum phase cycle of 128 accumulations for each mixing time, at short mixing times we obtained a signal-to-noise ratio of about 15 for polycarbonate and of more than 100 for the ^{13}C-enriched sites in the amino acids. The overall acquisition time for each sample covering 10 logarithmically spaced mixing times was about 2.5 h at each rotation speed. In addition, we used about 10 mg of methylmalonic acid as a sample with ^{13}C in natural isotopic abundance. All compounds except for PC were obtained commercially and used without further treatment.

APPENDIX

Under fast MAS, transverse magnetization can survive mixing times of even some tens of milliseconds, as it is evident from the long T_2 times in Fig. 4. We provide here an extended phase cycling that takes care of the proper cancellation of undesired transverse components during both t_m and t_z. The 180° pulses of the CODEX recoupling cycles have fixed phases according to the *xy*8 scheme (*41*) and will not be listed below. The terms "store" and "read-out" refer to the 90° pulses before and after the mixing time. "First" refers to the mixing time t_m between the evolution times, "second" to the second z-period, the z-filter t_z before data acquisition.

^{1}H-90°	$(+x\ -x)^{64}$
^{1}H-CP	$(+y)^{128}$
^{13}C-CP	$(+x)^{128}$
First store pulse	$((-y)^8(-x)^8(+y)^8(+x)^8)^4$
First read-out pulse	$((+y)^8(+x)^8)^2((-y)^8(-x)^8)^2$ $((-x)^8(+y)^8)^2((+x)^8(-y)^8)^2$
Second store pulse	$(-y)^{64}(-x)^{64}$
Second read-out pulse	$((+y)^2(-x)^2(-y)^2(+x)^2)^{16}$
Receiver	$((0\ 2\ 1\ 3\ 2\ 0\ 3\ 1)^2\ (2\ 0\ 3\ 1\ 0\ 2\ 1\ 3)^4$ $(0\ 2\ 1\ 3\ 2\ 0\ 3\ 1)^2)^2$

The first two steps in the phase cycle eliminate spurious signals from T_1 relaxation during the second z-period (t_z) and suppress directly excited ^{13}C signals by alternating the sign of the ^1H excitation pulse. The next three steps, which complete the first eight scans, cycle the second read-out pulse and the receiver but keep the second store pulse constant. This achieves CYCLOPS (*42*) phase cycling as well as the cancellation of transverse magnetization that might have survived t_z. The proper combination of signals is obtained in the next step ($\cos \Phi_1 \cdot \cos \Phi_2$ and $\sin \Phi_1 \cdot \sin \Phi_2$; see (*15, 16*)). The inversion of the first store pulse in concert with the receiver results in the removal of spurious signals from T_1 relaxation during t_m. Finally, the cancellation of transverse magnetization that might have survived the mixing time t_m (first z-period) is achieved by a fourfold cycling of the first read-out pulse.

ACKNOWLEDGMENTS

The authors thank Prof. Mei Hong for her generous help with the setup of the experiments. TJB and KSR acknowledge support by the Director for Energy Research, Office of Basic Energy Science, in the Materials Chemistry Program of Ames Laboratory, which is operated for the U.S. Department of Energy by Iowa State University under Contract W-7405-Eng-82. DR thanks the Deutsche Forschungsgemeinschaft DFG for financial support. The authors thank Prof. H. W. Spiess for making the ^{13}C-labeled polycarbonate available. TJB also acknowledges partial support by FAPESP (Brazil).

REFERENCES

1. W.-G. Hu and K. Schmidt-Rohr, Polymer ultradrawability: The crucial role of α-relaxation chain mobility in the crystallites, *Acta. Polym.* **50,** 271–285 (1999).
2. A. F. deJong, A. P. M. Kentgens, and W. S. Veeman, Two-dimensional exchange NMR in rotating solids. A technique to study very slow molecular reorientations, *Chem. Phys. Lett.* **104,** 337–342 (1984).
3. A. G. Palmer, J. Williams, and A. McDermott, NMR studies of biopolymers dynamics, *J. Phys. Chem.* **100,** 13293–13310 (1996).
4. D. E. Favre, D. J. Schaefer, S. M. Auerbach, and B. F. Chmelka, Direct measurement of intercage hopping in strongly adsorbing guest-zeolite systems, *Phys. Rev. Lett.* **81,** 5852–5855 (1998).
5. A. Gedeon, D. E. Favre, D. Reichert, J. MacNeil, and B. F. Chmelka, Distribution of site-hopping geometries and rates for benzene adsorbed on Ag–Y zeolite, *J. Phys. Chem. A* **103,** 6691–6703 (1999).
6. S. Hediger, L. Emsley, and M. Fischer, Solid-state NMR characterization of hydration effects on polymer mobility in onion cell-wall materials, *Carbohydr. Res.* **322,** 102–112 (1999).
7. C. Schmidt, B. Blümich, and H. W. Spiess, Deuteron two-dimensional exchange NMR in solids, *J. Magn. Reson.* **79,** 269–290 (1988).
8. A. Hagemeyer, K. Schmidt-Rohr, and H. W. Spiess, Two-dimensional nuclear magnetic resonance experiments for studying molecular order and dynamics in static and in rotating solids, *Adv. Magn. Reson.* **13,** 85–129 (1989).
9. J. J. Titman, Z. Luz, and H. W. Spiess, Solid-state reactions studied by carbon-13 rotor-synchronized magic-angle spinning two-dimensional exchange NMR. 2. The cope rearrangement and molecular reorientation in bullvalene, *J. Am. Chem. Soc.* **114,** 3765–3771 (1992).
10. K. Schmidt-Rohr and H. W. Spiess, "Multidimensional Solid-State NMR and Polymers" 1st ed., Chaps. 7–11, Academic Press, London, 1994.
11. E. R. deAzevedo, T. J. Bonagamba, and K. Schmidt-Rohr, Pure-exchange solid-state NMR, *J. Magn. Reson.* **142,** 82–96 (2000).
12. Y. Yang, M. Schuster, B. Blümich, and H. W. Spiess, Dynamic magic-angle spinning NMR spectroscopy: Exchange-induced sidebands, *Chem. Phys. Lett.* **139,** 239–243 (1987).
13. V. Gerardy-Montouillout, C. Malveau, P. Tekely, Z. Olender, and Z. Luz, ODESSA, a new 1D exchange experiment for chemically equivalent nuclei in rotating solids, *J. Magn. Reson.***123,** 7–15 (1996).
14. D. Reichert, H. Zimmermann, P. Tekely, R. Poupko, and Z. Luz, Time-reverse ODESSA. A 1D exchange experiment for rotating solids with several groups of equivalent nuclei, *J. Magn. Reson.* **125,** 245–258 (1997).
15. E. R. deAzevedo, W.-G. Hu, T. J. Bonagamba, and K. Schmidt-Rohr, Centerband-only detection of exchange: Efficient analysis of dynamics in solids by NMR, *J. Am. Chem. Soc.***121,** 8411–8412 (1999).
16. E. R. deAzevedo, W.-G. Hu, T. J. Bonagamba, and K. Schmidt-Rohr, Principles of centerband-only detection of exchange in solid-state NMR, and extension to four-time centerband-only detection of exchange, *J. Chem. Phys.* **112,** 8988–9001 (2000).
17. E. R. deAzevedo, S. B. Kennedy, and M. Hong, Determination of slow motions in extensively isotopically labeled proteins by magic-angle-spinning ^{13}C-detected ^{15}N exchange NMR, *Chem. Phys. Lett.* **321,** 43–48 (2000).
18. C. E. Bronniman, N. M. Szeverenyi, and G. E. Maciel, ^{13}C spin diffusion of adamantane, *J. Chem. Phys.* **79,** 3694–3700 (1983).
19. H. T. Edzes and J. P. C. Bernards, Two-dimensional exchange NMR in static powders—interchain C-13 spin exchange in crystalline polyethylene, *J. Am. Chem. Soc.* **106,** 1515–1517 (1984).
20. D. L. VanderHart, Natural-abundance ^{13}C–^{13}C spin exchange in rigid crystalline organic solids, *J. Magn. Reson.* **72,** 13–47 (1987).
21. H. H. Limbach, B. Wehrle, M. Schlabach, R. Kendrick, and C. S. Yannoni, CPMAS polarization transfer methods for superposed chemical exchnage and spin diffusion in organic solids, *J. Magn. Reson.* **77,** 84–100 (1988).
22. B. H. Meier, Polarization transfer and spin diffusion in solid-state NMR, *Adv. Magn. Opt. Reson.* **18,** 1–116 (1994).
23. P. Tekely, M. J. Potrzebowski, Y. Dusausoy, and Z. Luz, Measurement of spin diffusion and intermolecular distances between chemically equivalent nuclei in rotating solids, *Chem. Phys. Lett.* **291,** 471–479 (1998).
24. D. J. Schaefer, D. E. Favre, M. Wilhelm, S. J. Weigel, and B. F. Chmelka, Site-hopping dynamics of benzene adsorbed on Ca–LSX zeolite studied by solid-state exchange ^{13}C NMR, *J. Am. Chem. Soc.* **119,** 9252–9267 (1997).
25. D. Reichert, G. Hempel, H. Zimmermann, P. Tekely, R. Poupko, Z. Luz, D. E. Favre, and B. F. Chmelka, The dynamics of diphenoxydiphenylether as studied by carbon-13 tr ODESSA NMR, *Appl. Magn. Reson.* **17,** 315–327 (1999).
26. A. Krushelnitsky, D. Reichert, G. Hempel, V. Fetodov, H. Schneider, L. Yagodina, and A. Shulga, Superslow backbone protein dynamics as studied by 1D solid-state MAS exchange NMR spectroscopy, *J. Magn. Reson.* **138,** 244–255 (1999).
27. D. Reichert, G. Hempel, R. Poupko, Z. Luz, Z. Olejniczak, and P. Tekely, Carbon-13 spin exchange in durene as studied by MAS spectroscopy, *Solid State NMR* **13,** 137–148 (1998).
28. Z. Olender, D. Reichert, A. Mueller, H. Zimmermann, R. Poupko, and Z. Luz, Carbon-13 chemical-shift correlation, spin-diffusion and self diffusion in isotopically enriched tropolone, *J. Magn. Reson. A* **120,** 31–45 (1996).
29. P. Tekely, D. Reichert, H. Zimmermann, R. Poupko, and Z. Luz, Initial conditions for ^{13}C MAS NMR 1D exchange involving chemically equivalent and inequivalent nuclei, *J. Magn. Reson.* **145,** 173–183 (2000).
30. M. M. Maricq and J. S. Waugh, NMR in rotating solids, *J. Chem. Phys.* **70,** 3300–3316 (1979).
31. G. Williams and D. C. Watts, Non-symmetrical dielectric relaxation behavior arising from a simple empirical decay function, *Trans. Faraday Soc.* **66,** 80-85 (1970).

32. M. J. Potrzebowski, P. Tekely, and Y. Dusausoy, Comment to ^{13}C-NMR studies of α- and γ-polymorphs of glycine, *Solid State NMR* **11,** 253–257 (1998).
33. Y. Iitaka, The crystal structure of γ-glycine, *Acta Crystallogr*. **14,** 1–10 (1961).
34. Å. Kvick, W. M. Canning, T. F. Koetzle, and G. J. B. Williams, An experimental study of the influence of temperature on a hydrogen-bonded system: The crystal structure of γ-glycine at 83 K and 298 K by neutron diffraction, *Acta Crystallogr. B* **36,** 115–120 (1980).
35. P.-G. Jönsson and Å. Kvick, Precision neutron diffraction structure determination of protein and nucleic acid components: III. The crystal and molecular structure of the amino acid α-glycine, *Acta Crystallogr. B* **28,** 1827–1833 (1972).
36. K. Schmidt-Rohr and H. W. Spiess, "Multidimensional Solid-State NMR and Polymers," 1st ed., Chaps. 3 and 13, Academic Press, London, 1994.
37. R. Challoner, J. Kümmerlen, and C. A. McDowell, Spectral spin diffusion under n = 0 rotational resonance, *Mol. Phys.* **83,** 687–700 (1994).
38. A. Samoson, Advances in sample spinning technology: MAS at 50 kHz, 41st Experimental NMR Conference, Asilomar, CA (2000).
39. K. Saalwächter and K. Schmidt-Rohr, Relaxation-induced dipolar exchange with recoupling—An MAS NMR method for determining heteronuclear distances without irradiating the second spin, *J. Magn. Reson.* **145,** 161–172 (2000).
40. R. Tycko, D. P. Weliky, and A. D. Berger, Investigation of molecular structure in solids by two-dimensional NMR exchange spectroscopy with magic angle spinning, *J. Chem. Phys.* **105,** 7915–7930 (1996).
41. T. Gullion, D. B. Baker, and M. S. Conradi, New compensated Carr–Purcell sequences, *J. Magn. Reson.* **89,** 479–484 (1990).
42. E. O. Stejskal and J. Schaefer, Data routing in quadrature FT NMR, *J. Magn. Reson.* **13,** 249–251 (1974).